Am J Physiol Heart Circ Physiol 297: H811–H820, 2009.
First published June 26, 2009; doi:10.1152/ajpheart.00385.2009.

Speckle tracking echocardiography in the assessment of mouse models of cardiac dysfunction

Yu Peng,[1,4]* Zoran B. Popović,[1]* Nikolai Sopko,[3] Jeannie Drinko,[1] Zheng Zhang,[4] James D. Thomas,[1] and Marc S. Penn[1,2,3]

[1]*Department of Cardiovascular Medicine, Heart and Vascular Institute,* [2]*Skirball Laboratory for Cardiovascular Cellular Therapeutics, Center for Cardiovascular Cell Therapy, and* [3]*Department of Stem Cell Biology and Regenerative Medicine, Cleveland Clinic, Cleveland, Ohio; and* [4]*Department of Cardiology, The First Affiliated Hospital of Lanzhou University, Lanzhou, China*

Submitted 24 April 2009; accepted in final form 23 June 2009

Peng Y, Popović ZB, Sopko N, Drinko J, Zhang Z, Thomas JD, Penn MS. Speckle tracking echocardiography in the assessment of mouse models of cardiac dysfunction. *Am J Physiol Heart Circ Physiol* 297: H811–H820, 2009. First published June 26, 2009; doi:10.1152/ajpheart.00385.2009.—Two-dimensional (2-D) speckle tracking echocardiography (STE) accurately quantifies circumferential strain (S_{circ}) and radial strain (S_{rad}) in humans and in large and small animals. This study was performed to assess sensitivity of S_{circ} and S_{rad} to left ventricular (LV) dysfunction in mouse models. We performed 2-D and M-mode echocardiography *1*) in 6 mice during superficial and profound isoflurane anesthesia, *2*) serially in 12 mice to monitor the development of heart failure induced by transverse aortic constriction (TAC) and in 8 corresponding control mice, and *3*) in 26 mice with varying degrees of TAC-induced heart failure and 12 corresponding control mice immediately before euthanasia. Fractional shortening (FS) and LV mass were measured from standard M-mode tracings, whereas S_{circ} and S_{rad} were derived by STE. Percent fibrosis and myocyte diameters were assessed from whole heart cross-sectional specimens stained by Masson trichrome. Profound isoflurane anesthesia decreased S_{circ} ($P = 0.027$) but not S_{rad} ($P > 0.05$). Mice subjected to TAC showed an immediate and sustained decrease in FS ($P = 0.035$), S_{circ} ($P = 0.016$), and S_{rad} ($P = 0.012$). S_{circ} showed better correlation with FS ($r = 0.56$ and $P < 0.0001$) and LV mass ($r = 0.42$ and $P = 0.0003$) than S_{rad} ($r = 0.54$ and $P < 0.0001$ for FS and $r = 0.37$ and $P = 0.014$ for LV mass, respectively). Percent fibrosis correlated better with S_{circ} ($r = 0.46$ and $P = 0.004$) than with S_{rad} ($r = -0.32$ and $P = 0.05$), whereas myocyte diameter showed similar correlation with both strains ($r = 0.45$ and $r = -0.44$, respectively, and $P = 0.006$ for both). STE correctly identifies LV dysfunction and histological changes in mice and can be used for the serial assessment of cardiac remodeling in murine models.

transverse aortic constriction; systolic strain; systolic function

TWO-DIMENSIONAL (2-D) speckle tracking echocardiography (STE) is a novel technique that enables the assessment of myocardial strain through the analysis of speckle motion inherently present in a standard, 2-D echocardiographic image (18). In contrast to tissue Doppler-based assessment of strains, the STE process is angle independent and is less operator dependent. The STE technique has been validated in experimental and human studies and found to correspond well to established "gold standard" techniques (2, 7, 12).

With the increasing use of transgenic mice in cardiovascular research, the need for rapid and accurate assessment of global and segmental myocardial function has become apparent. However, in this setting, researchers are often offset by poor spatial and temporal resolution due to murine size and rapid heart rate. Researchers are often limited to the crudest of assessments, such as M-mode-derived measures of ventricular function. Thus, there is a constant and pressing need to maximize the utility of widely available clinical echocardiography systems for application in small animal cardiovascular research.

We (14) have recently shown STE can quantify circumferential strain (S_{circ}) and radial strain (S_{rad}) in rats. While STE has previously been reported in mice by several laboratories using dedicated micro-imaging ultrasound scanners (7, 8), the question arises as to whether it is possible to obtain similar results with conventional clinical echocardiography hardware and software. In this study, our primary aim was to test the sensitivity of strain measurement to changes in global left ventricular (LV) contractility in mouse models of LV dysfunction. For this purpose, we induced LV dysfunction either acutely by isoflurane inhalation (21) or by transaortic constriction (TAC) (20). Our secondary aim was to discern whether the changes that occur with progressive LV dysfunction induced by TAC are preceded by a LV mass increase or if the LV mass increase and LV dysfunction progress in parallel.

METHODS

All the animal experiments reported in this article were approved by the Institutional Animal Care and Use Committee of Cleveland Clinic and were in compliance with the National Institutes of Health *Guide for the Care and Use of Laboratory Animals*.

Experimental Protocols

We assessed 2-D echocardiographic LV short-axis images in three protocols. Fractional shortening (FS) and LV mass were measured from standard M-mode tracings, whereas S_{circ} and S_{rad} were derived by STE using Echopac PC software (GE Medical).

Protocol 1. We assessed six healthy C57/B6 mice during the induction of reversible systolic dysfunction. To do so, we subjected these mice first to a high dose (5%) and then to a low dose (2.5%) of isoflurane anesthesia.

Protocol 2. To assess longitudinal changes in cardiac function, we assessed 20 C57/B6 mice, 12 of which underwent TAC and 8 of which had a sham operation. Animals were followed by bimonthly echocardiography for at least 6 mo or until they died a natural death. At each time point, standard M-mode echocardiography parameters were assessed. Additionally, we used STE to obtain S_{circ} and S_{rad} at

* Y. Peng and Z. B. Popović contributed equally to this work.
Address for reprint requests and other correspondence: M. S. Penn, Skirball Laboratory for Cardiovascular Cellular Therapeutics, Center for Cardiovascular Cell Therapy, Dept.s of Cardiovascular Medicine and Stem Cell Biology and Regenerative Medicine, Cleveland Clinic, 9500 Euclid Ave., NE3, Cleveland, OH 44195 (e-mail: pennm@ccf.org).

three time points: early (3 ± 2 days), exactly at the midpoint of the followup of the individual mouse (95 ± 44 days), and at the last followup echocardiography (174 ± 73 days).

Protocol 3. To study the relationships between myocardial histology and ventricular function, we separately assessed an additional 26 C57/B6 mice with TAC and 12 C57/B6 sham-treated mice immediately before their euthanasia 4 wk after surgery.

TAC Model

Strain C57/B6 mice obtained from Jackson Laboratories were anesthetized via an intraperitoneal injection of a mixture of xylazine (5 mg/kg) and ketamine (80 mg/kg). Under a dissecting microscope (model M690-R, Leica), the animals were placed in a supine position, and their sternums were shaved and sterilized with alcohol. Animals were placed on a ventilator (Harvard Apparatus) with a respiratory rate of 105 breaths/min and a tidal volume of 0.25 ml and 60% oxygen. A sternotomy was performed, and the transverse aorta between the right subclavian and left common carotid arteries was isolated. A single 7-0 silk suture was placed around the transverse aorta and constricted against a 27-gauge needle placed externally on top of the aorta. After the suture had been tightened, the needle was removed, leaving the aorta ~75% occluded. Once banded, the sternum was closed with 6-0 silk suture, and the skin was closed with 6-0 prolene. Any residual pneumothorax was reduced using a 1-ml syringe with a 20-gauge needle before the skin was closed. Pulsed wave Doppler echocardiography performed 24 h after surgery showed that the pressure gradient across the constriction in all animals was at least 64 mmHg. In control age-matched mice, a sham operation without aorta occlusion was performed. After surgery, animals were assessed in an awake, nonsedated state on postoperative *days 1*, *13*, *21*, and *35* and then biweekly for a period of 6 mo or until they died spontaneously.

Echocardiographic Data Acquisition

Echocardiography was performed using a Vivid 7 ultrasound machine (GE Medical) equipped an il3L linear probe operated at 14 MHz. Mice were imaged in a conscious state at a room temperature of 73°F and with decreased ambient lighting while held by an experienced handler in a supine left decubitus postion. All mice underwent at least one echocardiography measurement to get used to the procedure.

The heart was imaged in the 2-D mode in the parasternal long- and short-axis views with a depth setting of 1.0 cm and at a frame rate of ≥275 frams/s. In *protocol 1*, the LV area was measured from short-axis views at papillary muscle levels, and the fractional area change (FAC) was calculated as follows: $FAC = (LVA_d - LVA_s)/LVA_d$, where LVA_d and LVA_s are the short-axis LV areas at diastole and systole, respectively. In *protocols 2* and *3*, an M-mode image was obtained at a sweep speed of 200 mm/s. Diastolic LV wall thickness, systolic LV wall thickness, LV end-diastolic dimension (LVEDD), and LV end-systolic chamber dimension (LVESD) were measured. All measurements were done from leading edge to leading edge according to American Society of Echocardiography guidelines (6). The percentage of LV FS was calculated as follows: FS (in %) = (LVEDD − LVESD)/LVEDD. LV mass was calculated using the following equation: LV mass (in mg) = $1.055\ [(LVEDD + PWT_d + VST_d)^3 - (LVEDD)^3]$, where 1.055 is the gravity of the myocardium, PWT_d is diastolic posterior wall thickness, and VST_d is diastolic ventricular septum thickness (3).

Speckle Tracking Assessment of Strains

2-D grayscale loops were acquired in the LV short-axis view at a frame rate of >275 frames/s except for *protocol 1*, where the frame rate was 375 frames/s for all of the data. For each experiment, at least three consecutive cardiac cycles were recorded and digitally stored on a hard disk for offline analysis on a workstation. We used a speckle-tracking algorithm incorporated into Echopac 7.070 software (GE Medical). The STE analysis was performed by the same trained observer. The region of interest was overlaid across a cross section of the ventricular silhouette at the image corresponding to the minimal endocardial area. The software algorithm then automatically divided the LV short-axis view into six segments for speckle tracking throughout the cardiac cycle. The tracking quality was then visually inspected, and, if it was satisfactory for at least five segments, the tracing was accepted.

Since most of our experiments were done in conscious mice without the possibility of registering the electrocardiogram, we modified the original process of detection of end systole and end diastole as follows. End diastole was defined as the first crossover point from blue to red in a radial velocities color M-mode map. This time point usually coincided with the crossover point of the global S_{circ} curve (Fig. 1). End systole was defined as the minimum LV short-axis area. Segmental S_{circ} and S_{rad} curves were then constructed by integrating the appropriate signals starting from the end-diastolic points and then averaged to obtain average segmental strain curves. End-systolic strains were then obtained from the average strain curve. The mean value was used for statistical analysis.

Quantifying Observer Variability

To estimate inter- and intraobserver variability, we used data obtained in six mice, three of which were sham treated. To estimate intraobserver variability, the same observer applied speckle tracking software twice to the same cardiac cycle; the same procedure was used to assess interobserver variability. Data are presented as means of the absolute differences between measurements and by the correlation coefficient (r).

Histological Analysis

Mice were euthanized [KCl (2 meq iv) to arrest the heart in diastole] under deep anesthesia. Hearts were harvested, and LVs were dissected. After the LV weight had been measured to the 10th of a milligram on a Mettler balance, hearts were fixed in 10% paraformaldehyde and paraffinized. Short-axis sections (5 μm) were cut, and Masson's trichrome staining for collagen was performed. Whole sections were imaged at ×200 magnification via bright-field microscopy (DM5000B, Leica). Cardiomyocyte diameters were measured using the transnuclear width of at least 35 myocytes (1). Cardiac fibrosis was assessed by measuring the collagen-stained area as a percentage of the total myocardial area. All quantitative evaluations were performed with ImagePro Plus software (version 61.0.346, Media Cybernetics) (1).

Statistical Analysis

Data are presented as means ± SD unless otherwise noted. To assess whether longitudinal changes in ventricular function could be assessed from a limited number of strain data points, we calculated individual (within animal) slopes of the relationship between time after surgery and FS, LV mass, S_{circ}, or S_{rad} using simple linear regression. Whereas an average of 17 ± 6 data points was used to construct the "reference" standard of time-FS and time-LV mass slopes, only 3 data points were used to construct time-strain slopes.

Paired comparisons were performed by the Wilcoxon paired test. Correlations were assessed by Pearson's r values. The comparison of r values was done using SISA online software (19). Between-group differences were assessed by Student's t-test or one-way ANOVA as appropriate. Serial changes during the early postconstriction period were assessed by repeated-measures ANOVA, with posthoc compar-

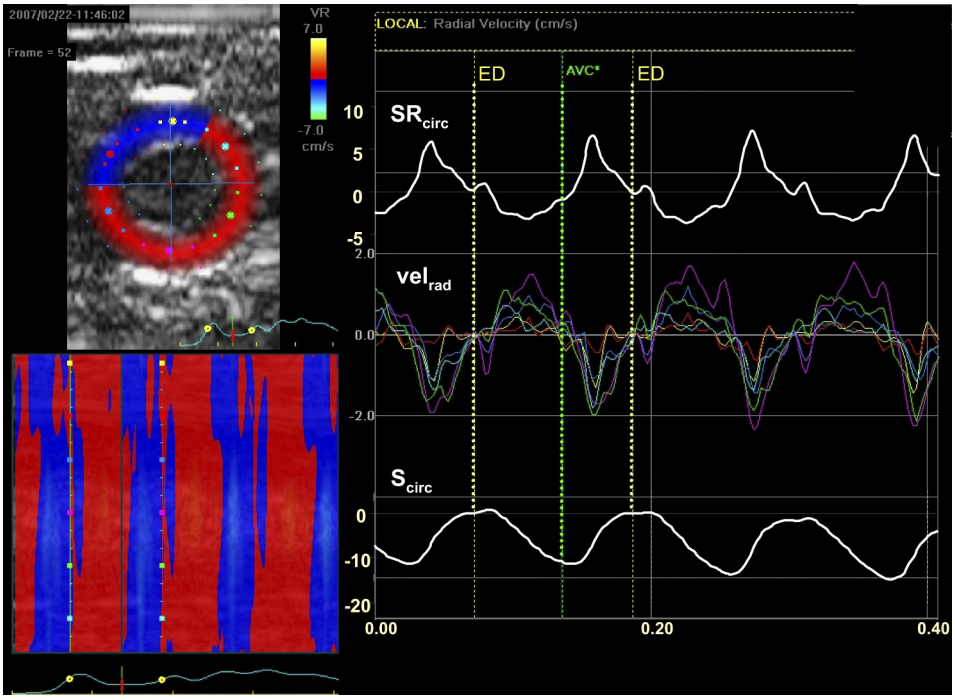

Fig. 1. Selection of end diastole (ED) and end systole (ES) to determine left ventricular (LV) circumferential strain (S_{circ}) and radial strain (S_{rad}) by two-dimensional speckle tracking echocardiography. ED was defined as a crossover point from blue to red in a radial velocity (vel_{rad}) color M-mode map and usually coincided with the crossover points of the global S_{circ} rate (SR_{circ}) curve (*top* trace) and of the segmental vel_{rad} curves (*middle* traces). Please note that in some regions of the color M-mode map, the red color during systole was briefly interrupted by a narrow strip of blue corresponding to the end of isovolumic contraction, which was, in turn, followed by a constant red color, indicating ejection. ES was defined as the minimal LV cross-sectional area and usually coincided with the end of the systolic wave of the global SR_{circ} curve and of the segmental vel_{rad} curves. The yellow and green vertical lines represent ED and ES, respectively. AVC, aortic value closure. S_{circ} curve shown on the *bottom* trace.

isons performed by Student's *t*-test with the Bonnferonni correction. *P* values of <0.05 were considered statistically significant.

RESULTS

Assessment of Strain Sensitivity to Acute Changes in LV Systolic Function

Compared with conscious state data, low-dose isoflurane significantly increased R-R intervals (136 ± 28 vs. 94 ± 9 ms, $P = 0.01$) without affecting FAC (0.59 ± 0.10 vs. 0.63 ± 0.11, $P > 0.1$). In all six mice, acute LV dysfunction induced by high-dose isoflurane consistently induced decreased FAC and increased the LV end-systolic area ($P = 0.027$ vs. control for both; Fig. 2, *A* and *B*). Similarly, LV dysfunction consistently decreased the absolute values of S_{circ} ($P = 0.027$ vs. control; Fig. 2*C*). S_{rad}, however, did not decrease during LV dysfunction at this dose of anesthesia ($P > 0.05$ vs. control; Fig. 2*D*). Overall, FAC inversely correlated with S_{circ} ($r = -0.67$, $P = 0.017$) and showed a trend for correlation with S_{rad} ($r = 0.45$, $P = 0.14$).

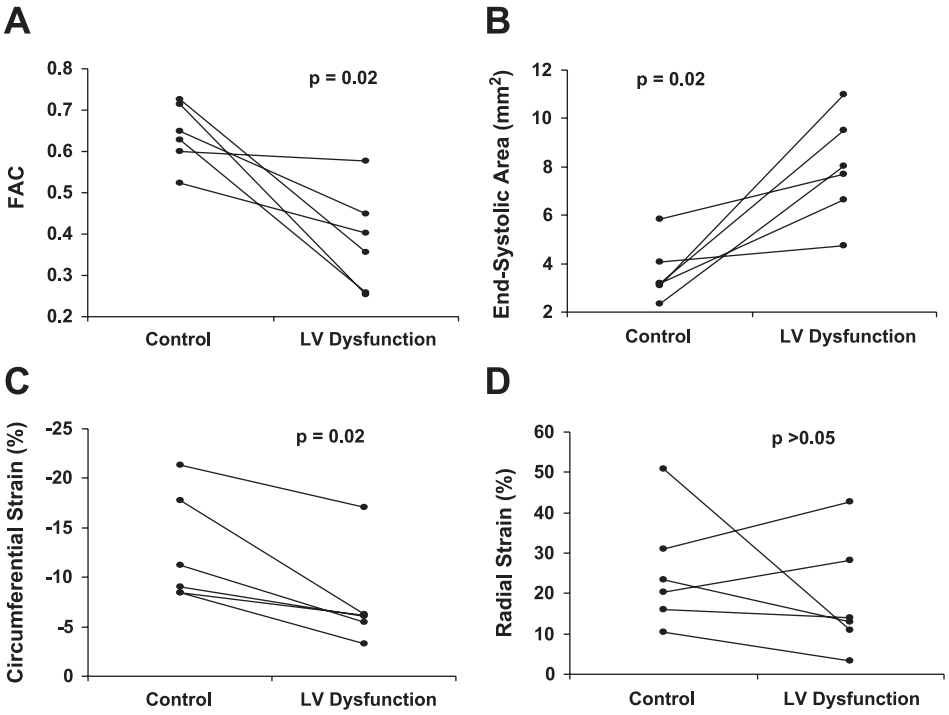

Fig. 2. Impact of acute LV dysfunction induced by a high dose of isoflurane on fractional area change (FAC; *A*), LV end-systolic area (*B*), S_{circ} (*C*), and S_{rad} (*D*).

Impact of TAC on S_{circ} and S_{rad}

In each of 20 mice (12 mice with TAC and 8 mice with sham operation), we analyzed the data obtained 3 ± 2 days (early), 95 ± 44 days (midterm), and 174 ± 73 days (late) after surgery. Additional experiments were analyzed in three mice. As expected, the LV mass was greater in banded mice (P = 0.01), with the difference between the two groups increasing over time (P = 0.004). This was associated with lower FS, and S_{circ} and S_{rad} in banded animals appeared consistent throughout the study period. Mice subjected to TAC showed an immediate and sustained decrease in FS (P = 0.035), S_{circ} (P = 0.016), and S_{rad} (P = 0.012) throughout the study period (Fig. 3, *A–C*). This indicates that the measurement of strain in mice is sensitive enough to detect a difference in contractility between relatively small animal groups. S_{circ} showed correlations with FS (r = −0.56 and P < 0.0001) and LV mass (r = 0.42 and P = 0.0003) that were similar to S_{rad} (r = 0.54 and P < 0.0001 for FS and r = −0.37 and P = 0.014 for LV mass; Fig. 4).

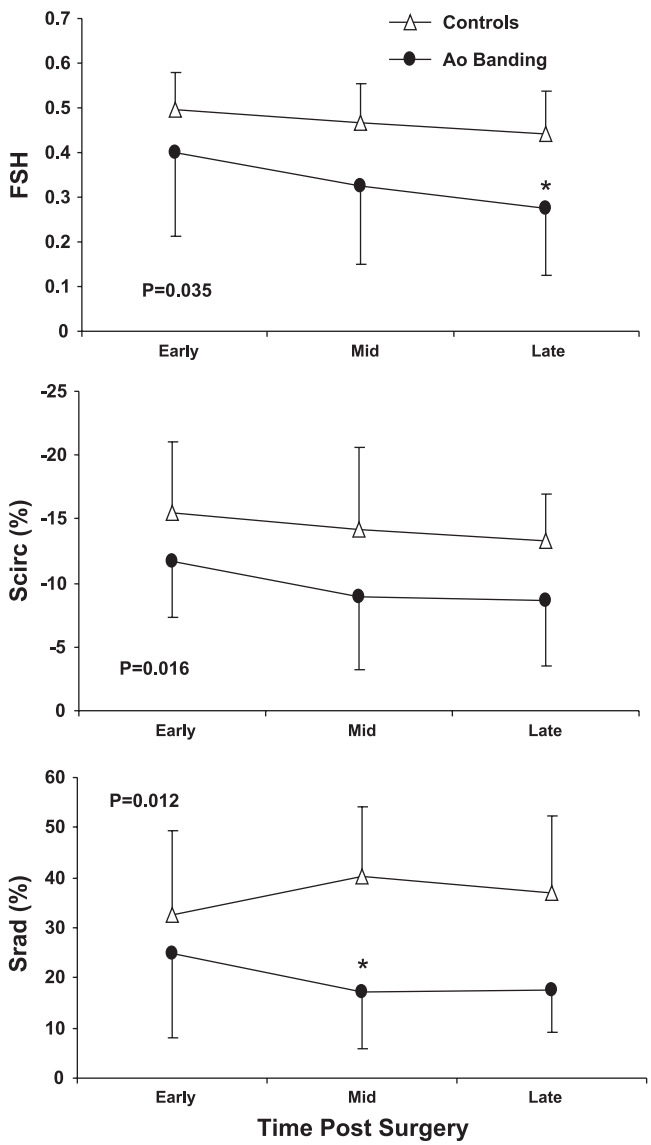

Fig. 3. Changes in fractional shortening (FS) and LV strains 3 ± 2 days (early), 95 ± 44 days [midterm (mid)], and 174 ± 73 days (late) after transaortic constriction [TAC; aortic banding (Ao banding)]. *P < 0.05 vs. sham-operated mice (controls) at a particular time point.

Longitudinal Assessment of LV Function After Aortic Constriction

Previous studies have shown that the LV mass continually increases after aortic constriction, whereas systolic function decreases at a rate that varies between animals. Our aim was to assess if it was possible to model changes in LV mass and systolic function by simple linear regression. However, under some protocols, aortic constriction reversibly decreases systolic function during the first postoperative week (10). This would indicate that one would have to exclude early data from the analysis, although they may be crucial from an experimental standpoint. For this reason, our experiment included an assessment of whether or not reversible systolic dysfunction occurred. During the first 35 postoperative days, FS was uniformly lower in banded animals (P = 0.037), with a weak linear trend toward decreasing FS during early followup (P = 0.1). In contrast, LV mass showed only a trend toward a difference between the two groups (P = 0.07). However, LV mass increased linearly during followup in banded animals (P = 0.0001), whereas it remained unchanged in sham-treated animals (P = 0.93; Table 1). These data indicate that the homeometric phenomenon is operative early after TAC (5) and that a linear model of LV function change, postconstriction, could be applied even early after surgery.

We then compared the sensitivity of different systolic function-time relationships to within-animal changes in contractility. Figure 5 shows an example of individual data points and corresponding slopes of function-time relationship derived in a single banded animal. There was a noticeable constant trend toward a LV mass increase with a parallel decrease of all three parameters of systolic function.

The average slope of the LV mass increase over the study period was 1.4 mg/day (range: 0.2 to 6.6 mg/day) in TAC animals and 0.03 mg/day (range: −0.23 to 0.2 mg/day) in controls (P = 0.02). The average slope of the FS decrease was -1.7×10^{-3}/day (range: -6.0×10^{-3}/day to 0.4×10^{-3}/day) in TAC animals and -0.2×10^{-3}/day (range: -0.6×10^{-3}/day to 0.8×10^{-3} g/day) in controls (P = 0.044). Slopes of time-strain relationships calculated from only three data points correlated well with the "reference" standard slopes of time-FS and time-LV mass relationships obtained from multiple (17 ± 6) data points. However, slopes of the S_{circ} decrease showed a better correlation with slopes of the LV mass increase (r = 0.88) and FS decrease (r = −0.76) than did the slopes of the S_{rad} decrease (r = −0.55 and r = 0.61 with slopes of the LV mass increase and FS decrease, respectively, P = 0.004 and P = 0.1 vs. S_{circ} for the difference in absolute r values).

Echocardiography and Histomorphometric Characteristics

To validate the echo-derived estimates of LV mass, the true LV mass determined in each of the 38 mice studied under *protocol 3* was compared with the echo-derived LV mass determined just before euthanasia. The r value of 0.82 (P < 0.0001) indicated a strong correlation between true and mea-

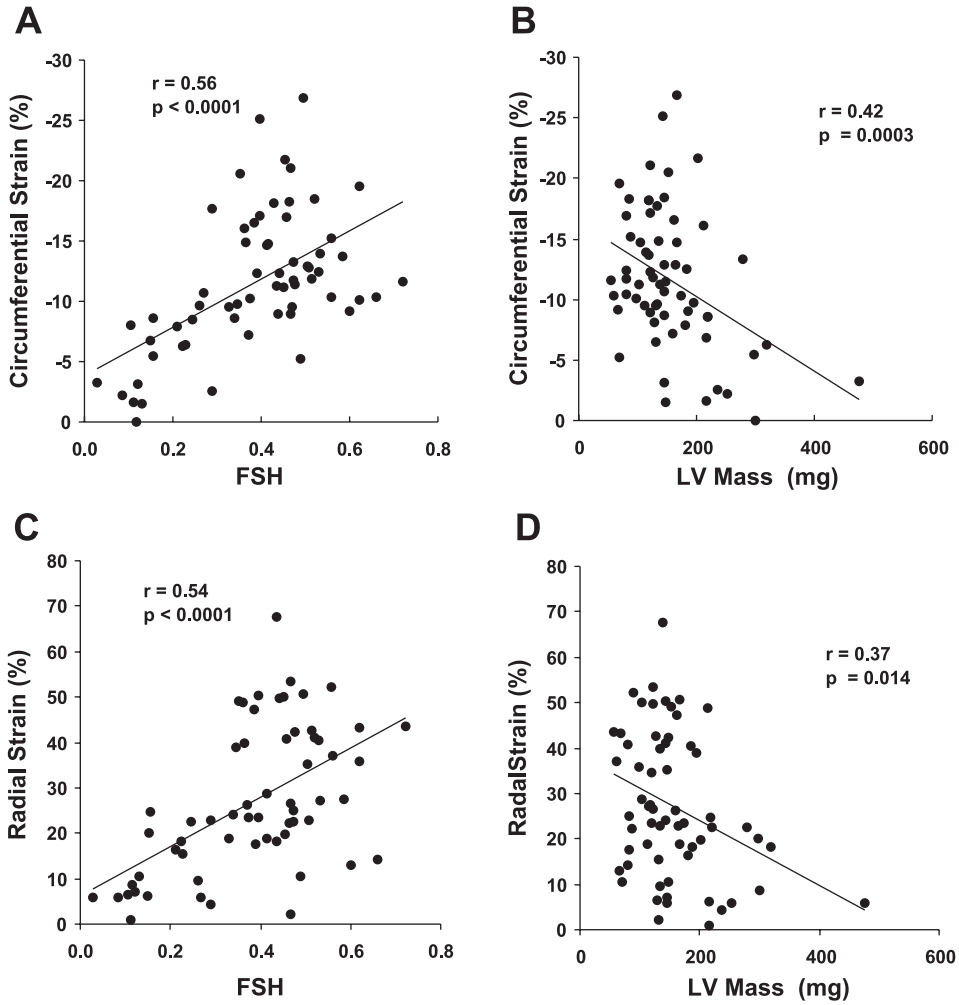

Fig. 4. *A* and *B*: correlations between S_{circ} and FS (*A*) and LV mass (*B*). *C* and *D*: correlations between S_{rad} and FS (*C*) and LV mass (*D*).

sured mass (Supplemental Fig. 1).[1] Figure 6 shows characteristic echocardiographic and histological data of these mice (12 control mice and 26 mice after TAC) 4 wk after surgery. Correlations between cardiac function parameters (FS, S_{circ}, and S_{rad}) and true LV mass and histology in TAC and control mice are shown in Fig. 7. FS correlated moderately with true LV mass, but did not correlate with percent fibrosis, and showed a weak correlation with myocyte diameter (Fig. 7, *A–C*). S_{circ} correlated moderately strongly with true LV mass and showed moderate correlations with both percent fibrosis and myocyte diameter (Fig. 7, *D–F*). Finally, S_{rad} correlated moderately strongly with true LV mass but showed a weak correlation with percent fibrosis and a moderate correlation with myocyte diameter (Fig. 7, *G–I*).

Observer Variability Data

Intra- and interobserver variability data are shown in Table 2. The interobserver variability of global strain in mice was roughly two times lower than the segmental strain variability observed in rats, where the mean absolute difference for same-cycle intraobserver measurements was 2.7 ± 2.2% and 8.6 ± 6.8% for S_{circ} and S_{rad}, respectively (14).

[1] Supplemental Material for this article is available online at the *American Journal of Physiology-Heart and Circulatory Physiology* website.

Table 1. *Early postoperative changes in LV mass and systolic function after TAC*

	Day 1		*Day 13*		*Day 21*		*Day 35*	
	Sham	TAC	Sham	TAC	Sham	TAC	Sham	TAC
n	8	12	8	12	8	12	8	12
FS	0.5±0.02	0.43±0.05	0.59±0.04	0.37±0.07	0.46±0.02	0.37±0.05‡	0.47±0.04	0.35±0.06
LV mass, mg	122±12	102±10	109±6	149±14*	135±13	173±15†	118±13	173±17†

Data are means ± SD; *n*, number of animals. LV mass, left ventricular (LV) mass after M-mode echocardiography; TAC, transverse aortic constriction; sham, sham operation; FS, fractional shortening. *$P < 0.05$ and †$P < 0.01$ vs. the initial LV mass; ‡$P < 0.05$ vs. sham animals.

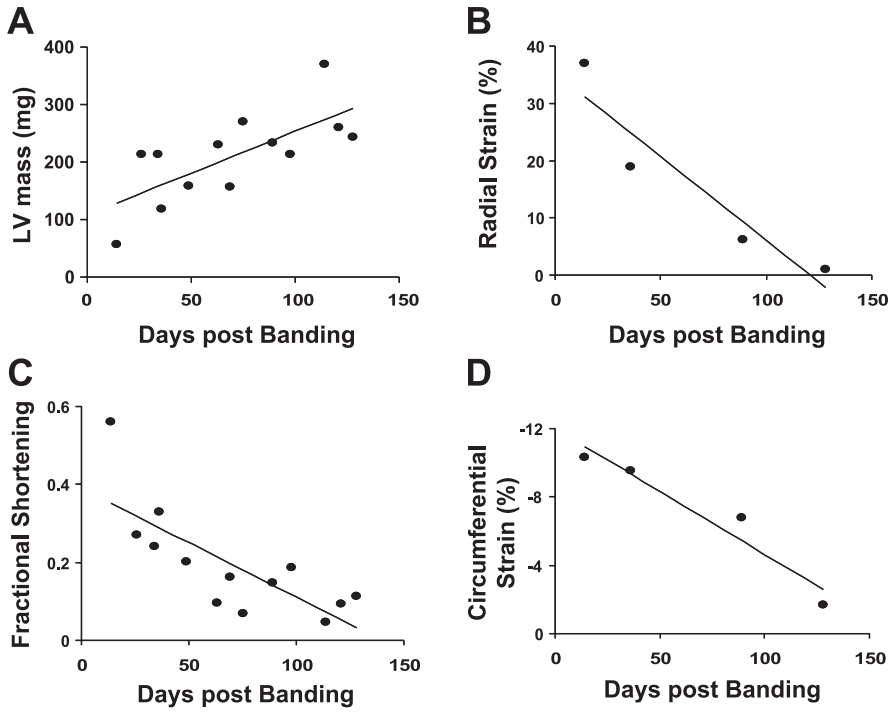

Fig. 5. Example of parallel worsening of FS (*C*), S_{rad} (*B*), and S_{circ} (*D*) with an increase of LV mass (*A*) obtained in a single TAC animal (a fourth data point in the strain data is for illustrative purposes only).

DISCUSSION

In this study, we used a semiautomated quantitative method of STE to assess S_{circ} and S_{rad} in murine models of LV dysfunction. We have shown that speckle tracking-derived global S_{circ} is sensitive to both acute and chronically induced LV dysfunction in mice. S_{rad}, however, was sensitive to chronic but not acute LV dysfunction. Additionally, we found that changes in S_{circ} are a slightly more sensitive descriptor of functional worsening that leads to TAC-induced heart failure and correlated better with the TAC-induced increase in fibrosis. These findings are in accordance with our previously published study (14) in which we showed that S_{circ} is more sensitive than S_{rad} to segmental fibrosis induced by myocardial infarction in a rat model of ischemic cardiomyopathy.

Measuring Strain: Tissue Doppler Versus Speckle Tracking

Several previous studies have used tissue Doppler echocardiography obtained by commercially available equipment to show that the S_{rad} rate in mice correlates with invasive measures of systolic function (11) and is a predictor of infarct transmurality when applied early after coronary artery occlusion (15, 17). However, although Doppler imaging has better temporal resolution than speckle tracking, it has several drawbacks. Due to Doppler angle dependency, only S_{rad}/strain rates can be obtained and only in the anterior and posterior LV segments. In this aspect, speckle tracking, with the ability to assess all segments by both strain components, is superior. Furthermore, Doppler-derived strain is obtained by subtracting tissue velocities recorded from two sampling regions. With currently available technology, the minimal distance between two sampling regions is 0.35 mm, the minimal sampling region is >0.2 mm (17), and the minimal wall thickness across which Doppler-derived S_{rad} can be obtained is >0.75 mm, which is close to the normal mouse LV wall thickness. While there are several small, proof-of-concept studies that have used custom-developed software and expensive dedicated small animal ultrasound machines to obtain or validate strain by speckle tracking in mice (7–9), these methods have yet to fully penetrate into a standard research arena.

Strain in the Assessment of Disease Progression in Mouse Models of Heart Failure

Heart failure syndrome, if untreated, is a progressive phenomenon that includes changes in physiology, cellular biology, and neurohormonal regulation irrespective of the initial etiology. In mice, almost universally, heart failure progression is assessed by M mode-derived FS. This method is simple and fast, but imprecise. For this reason, in clinical medicine, it was largely replaced by 2-D echocardiography almost 2 decades ago. However, assessing LV volumes by 2-D echocardiography is cumbersome and necessitates certain knowledge and experience. The assessment of strain by speckle tracking is a semiautomated process whose speed depends more on the quality of the image and hardware than on the operator. We have shown that changes in S_{circ} and S_{rad} obtained by this method accurately reflect changes in pathophysiology that occur during the evolution of TAC-induced heart failure. The TAC group had sustained LV contractile dysfunction that was apparent even during the first 35 days. During the followup of up to 180 days, we observed a progressive worsening in LVESD, FS, and LV mass, demonstrating continuous pathological remodeling (Fig. 2). We also observed an increase of interstitial fibrosis in TAC mice that the paralleled worsening of ventricular function (Fig. 3). Thus, the classical triad of pathological remodeling in heart failure (dilation, hypertrophy, and fibrosis) was present in this chronic small animal heart failure model. The rate of heart failure progression throughout the study period was constant and could be modeled as a linear

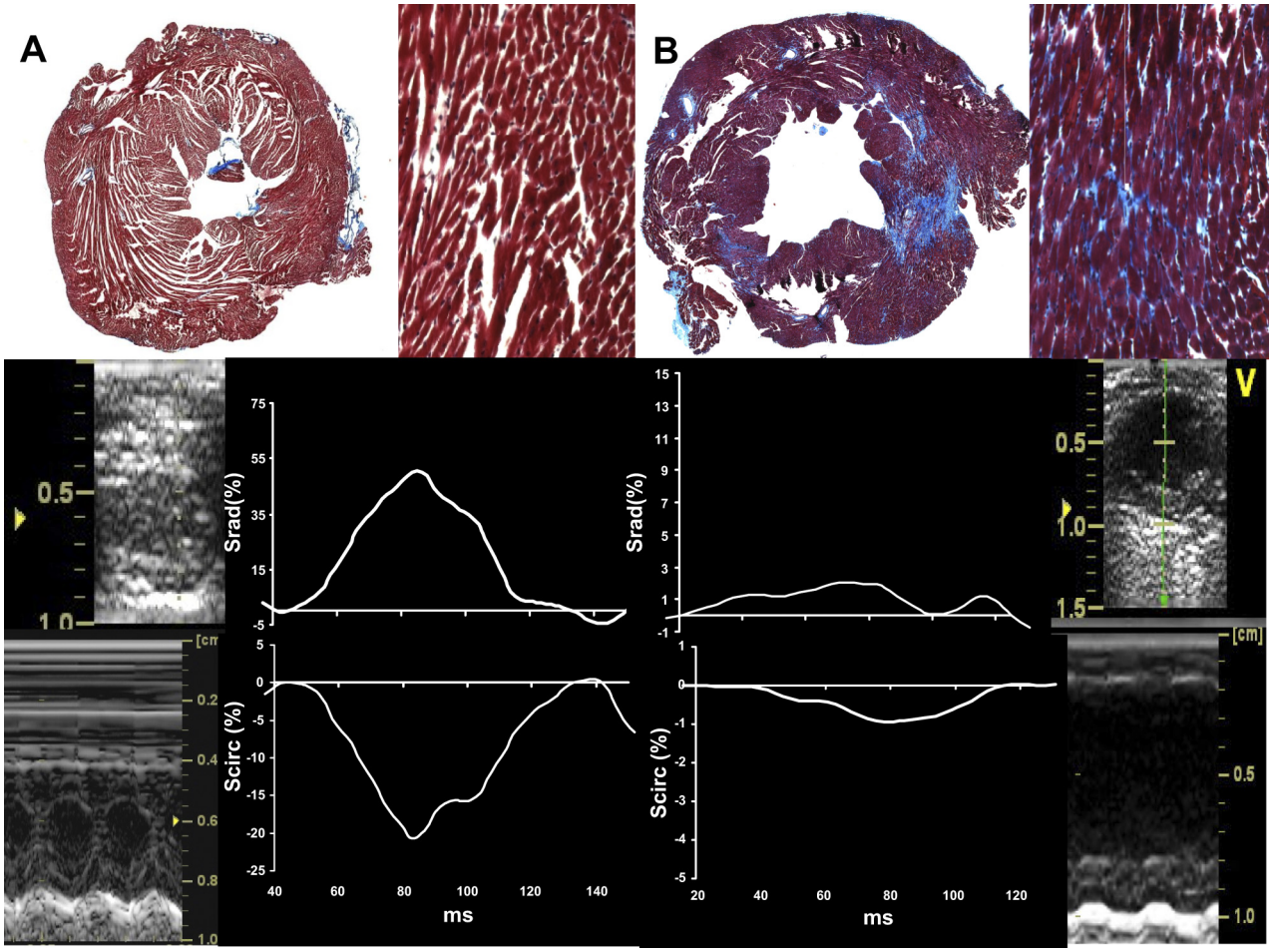

Fig. 6. *A*, *top left*: representative LV cross section of a control heart. *Top right*, LV cross section of control heart showing collagen density (stained by Masson trichrome). *Bottom*, corresponding echocardiographic short-axis views of the same heart (*left*) and corresponding segmental waveforms of systolic S_{circ} and S_{rad} (*right*). *B*, *top left*: representative LV cross section of a heart after TAC. *Top right*, collagen density staining of a LV cross section after TAC showing fibrosis (in blue). *Bottom*, corresponding echocardiographic short-axis views (*left*) and corresponding segmental waveforms of systolic S_{circ} and S_{rad} (*right*).

decrease of parameters of systolic function (FS, S_{circ}, and S_{rad}) and as a linear increase of LV mass. However, the rate of heart failure progression was variable between animals. Importantly, the rate of S_{circ} worsening showed better correlation with worsening of LV mass and FS than the rate of S_{rad} worsening.

The close relationships between LV mass, FS, S_{circ}, and S_{rad} indicate that strain measurements based on speckle tracking are able to detect LV dysfunction. Furthermore, our data show that by using speckle tracking, it is possible to reduce the number of serial measurements needed to assess the rate of progression of heart failure.

Strain Versus Histology in TAC

Fibrosis is one of the most important myocardial histological parameters, as it is related to myocardial viability, propensity for arrhythmias, and survival. Strain assessment was proposed as one of the possible methods to estimate fibrosis burden. As fibrosis represents a loss of functional myocardial tissue, the amount of fibrosis should directly correlate with the quantitative loss of function. Indeed, we show here that even relatively small amount of TAC-induced myocardial fibrosis leads to a significant decrease of strains, especially its circumferential component. In a previous rat study (14), we also noted that segmental fiborsis better correlated with S_{circ} than with S_{rad}. In contrast, FS appeared not to be affected by TAC-induced fibrosis in this model.

Both strain components as well as FS were sensitive to cardiomyocyte diameter and the LV mass increase. Interestingly, both S_{circ} and S_{rad} correlated better with true LV mass than with myocyte diameter. This can be explained by the fact that cardiomyocyte diameter is a function of both myocardial hypertrophy and ventricular dilation, which have opposing effects. Of note, the relationship between myocardial fibrosis and ventricular function is also not necessarily a one-to-one process, as the deterioration of ventricular function induced by extreme TAC can be so rapid that minimal fibrosis is associated with it.

Practical Implications

We believe that the strongest practical implication of this study would be to make quantitative strain measurements available to a larger number of researchers through the use of clinical ultrasound hardware and software that already enjoys a large presence in the medical ultrasound community. Although special equipment for mouse echocardiography is evolving, and even now has a superior special resolution than the

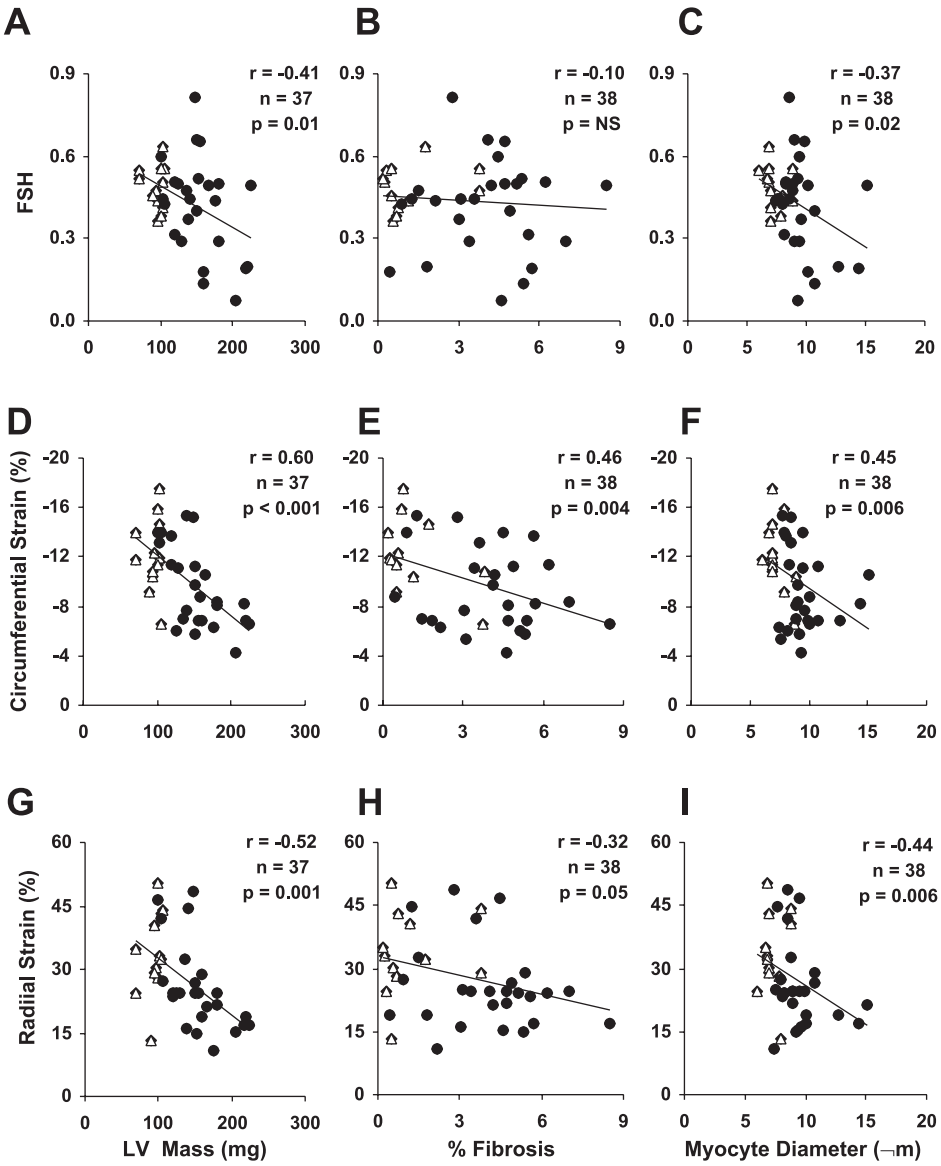

Fig. 7. Correlation between the LV functional parameters of FS (*A–C*), S_{circ} (*D–F*), and S_{rad} (*G–I*) and the morphological parameters of measured LV mass (*A*, *D*, and *G*), percent fibrosis (*B*, *E*, and *H*), and myocyte diameter (*C*, *F*, and *I*). S_{circ} showed the strongest correlation with all three morphological parameters, followed by S_{rad} and FS. △, Sham-operated mice; ●, mice that underwent TAC. NS, not significant. Please see text for details.

equipment we used, it will simply be out of reach for most small animal researchers.

Additionally, we have shown that even with a limited number of experiments, one can use STE to track changes in LV function to the same extent as with 5–10 times more frequent M-mode studies. Furthermore, the ability to completely automate data acquisition is very appealing. Indeed, software exists that can automatically track the speckle motion within a fixed region of interest (such as a circle). If one automates speckle tracking and applies it to an analysis of multiple consecutive beats, which is feasible given the constant increase of computer power, researchers will obtain a powerful, new, nonoperator-dependent tool.

Table 2. *Intra- and interobserver variability for circumferential and radial strain measurements*

	Circumferential Strain	Radial Strain
Mean	−11.4±7.9	31.2±16.5
Intraobserver variability		
Mean absolute difference, %	1.6±1.7	3.8±4.5
Correlation	0.99	0.95
Interobserver variability		
Mean absolute difference, %	3.7±4.2	5.3±4.1
Correlation	0.89	0.97

Values are means ± SE.

Another promising application of myocardial strain is in the segmental assessment of LV function in a murine model of chronic ischemic cardiomyopathy. Although the current echocardiographic quality of clinical echocardiography systems probably cannot sustain partitioning LV cross-sectional image into six segments as performed in larger animals, Li et al. (7) recently demonstrated that this could be accomplished in postinfarct mice using a dedicated small animal ultrasound micro-imaging system. It is anticipated that forthcoming improvements in the spatial resolution of small intraoperative transducers will make similar segmentations of the murine heart feasible on clinical ultrasound systems in the near future. Interestingly, S_{rad} was not sensitive enough to detect acute

ventricular dysfunction and was less sensitive than S_{circ} even in TAC-induced dysfunction. A probable explanation is that the utility of speckle tracking depends heavily on LV wall thickness relative to the resolution of the echo system. LV wall thickness is already small in mice and becomes even smaller in acute dysfunction. Additionally, a clinical study (2) has shown that S_{rad} suffers from limited reproducibility, thus indicating its more ancillary role in detecting LV dysfunction.

Finally, future work will almost certainly encompass the assessment of systolic and diastolic strain rates. Diastolic strain rates may be used as an additional surrogate of ventricular fibrosis (13) and segmental relaxation abnormalities (4). Currently, a major drawback in assessing strain rate is the frame rate. However, even with current equipment, one can obtain 2-D frame rates of close to 500 frames/s in smaller regions of interest, which seems satisfactory for obtaining relevant strain rates in mice (15). Li et al. (7) recently used a micro-imaging system and custom speckle tracking software to determine systolic strain rates in normal and postinfarct mice.

Limitations

This small study involved only 64 animals. Furthermore, we assumed that TAC has a uniform impact on all ventricular segments. The frame rates of 272–375 frames/s obtained in this study correspond to a relative sampling rate of 26–35 frames/cardiac cycle. Although in our previous rat study we successfully assessed segmental LV strains with only 18 frames/cardiac cycle, these numbers are still smaller than what is accomplished in clinical studies (16). Additionally, in clinical echocardiography, frame rates of >90 frames/s often lead to poor speckle tracking (16). However, the phased array transducers used in clinical studies have a degraded ultrasound image at >90 frames/s, due to the decrease of a number of scan lines (i.e., loss of a horizontal resolution) and an increase and blurring of speckles. With our 14-MHz linear transducer, the speckle size obtained when the mouse heart was imaged at 275 frames/s with a field width/depth setup of 1×1 cm was exactly the same as the speckle size obtained when the rat heart was imaged at the same frequency, at 123 frames/s, and at a field width/depth of 2×2 cm, i.e., the one we use in our previous article. Still, the relative speckle size was larger in the mouse heart than in the rat heart, which remains a limitation of this study. However, we tried to offset this by using an averaged, instead of segmental, strain signal.

Since in longitudinally followed mice banded animals had a shorter followup (143 ± 75 vs. 210 ± 14 days) as they were dying of heart failure, there is an imbalance in the followup dates. However, excluding animals with the shorter followup would have eliminated the most affected mice, whereas shortening the followup in the banded mice who survived for a longer period of time and developed LV hypertrophy and heart failure later in the course would have artificially decreased the between-group difference.

Finally, no comparison was made with an independent gold standard such as sonometric crystal implantation or MRI, as in a previous report (7). Thus, the actual precision of our measurements is unknown. However, the primary focus of this report was the sensitivity of strain measurements to pathology and the time course of heart failure development. Further studies that involve a larger number of animals and heart failure models with heterogeneity of ventricular function are needed.

Conclusions

In conclusion, we have shown that, in mice, speckle tracking-derived global S_{circ} efficiently detects acute and chronic LV dysfunction, accurately tracks the progression of TAC-induced heart failure, and is reflective of the fibrotic changes induced by TAC. On the other hand, global S_{rad} was less sensitive to the progression of heart failure, poorly reflected acute LV dysfunction, and showed little concordance with TAC-induced fibrosis. Further studies are needed to corroborate these findings in a larger number of animals and in a wider variety of murine models of LV dysfunction.

REFERENCES

1. **Bian J, Popovic ZB, Benejam C, Kiedrowski M, Rodriguez LL, Penn MS.** Effect of cell-based intercellular delivery of transcription factor GATA4 on ischemic cardiomyopathy. *Circ Res* 100: 1626–1633, 2007.
2. **Cho GY, Chan J, Leano R, Strudwick M, Marwick TH.** Comparison of two-dimensional speckle and tissue velocity based strain and validation with harmonic phase magnetic resonance imaging. *Am J Cardiol* 97: 1661–1666, 2006.
3. **Devereux RB, Alonso DR, Lutas EM, Gottlieb GJ, Campo E, Sachs I, Reichek N.** Echocardiographic assessment of left ventricular hypertrophy: comparison to necropsy findings. *Am J Cardiol* 57: 450–458, 1986.
4. **Firstenberg MS, Greenberg NL, Smedira NG, Castro P, Thomas JD, Garcia MJ.** The effects of acute coronary occlusion on noninvasive echocardiographically derived systolic and diastolic myocardial strain rates. *Curr Surg* 57: 466–472, 2000.
5. **Klautz RJ, Teitel DF, Steendijk P, van Bel F, Baan J.** Interaction between afterload and contractility in the newborn heart: evidence of homeometric autoregulation in the intact circulation. *J Am Coll Cardiol* 25: 1428–1435, 1995.
6. **Lang RM, Bierig M, Devereux RB, Flachskampf FA, Foster E, Pellikka PA, Picard MH, Roman MJ, Seward J, Shanewise JS, Solomon SD, Spencer KT, Sutton MS, Stewart WJ.** Recommendations for chamber quantification: a report from the American Society of Echocardiography's Guidelines and Standards Committee and the Chamber Quantification Writing Group, developed in conjunction with the European Association of Echocardiography, a branch of the European Society of Cardiology. *J Am Soc Echocardiogr* 18: 1440–1463, 2005.
7. **Li Y, Garson CD, Xu Y, Beyers RJ, Epstein FH, French BA, Hossack JA.** Quantification and MRI validation of regional contractile dysfunction in mice post myocardial infarction using high resolution ultrasound. *Ultrasound Med Biol* 33: 894–904, 2007.
8. **Luo J, Fujikura K, Homma S, Konofagou EE.** Myocardial elastography at both high temporal and spatial resolution for the detection of infarcts. *Ultrasound Med Biol* 33: 1206–1223, 2007.
9. **Luo J, Konofagou EE.** High-frame rate, full-view myocardial elastography with automated contour tracking in murine left ventricles in vivo. *IEEE Trans Ultrason Ferroelectr Freq Control* 55: 240–248, 2008.
10. **Nakamura A, Rokosh DG, Paccanaro M, Yee RR, Simpson PC, Grossman W, Foster E.** LV systolic performance improves with development of hypertrophy after transverse aortic constriction in mice. *Am J Physiol Heart Circ Physiol* 281: H1104–H1112, 2001.
11. **Neilan TG, Jassal DS, Perez-Sanz TM, Raher MJ, Pradhan AD, Buys ES, Ichinose F, Bayne DB, Halpern EF, Weyman AE, Derumeaux G, Bloch KD, Picard MH, Scherrer-Crosbie M.** Tissue Doppler imaging predicts left ventricular dysfunction and mortality in a murine model of cardiac injury. *Eur Heart J* 27: 1868–1875, 2006.
12. **Notomi Y, Lysyansky P, Setser RM, Shiota T, Popovic ZB, Martin-Miklovic MG, Weaver JA, Oryszak SJ, Greenberg NL, White RD, Thomas JD.** Measurement of ventricular torsion by two-dimensional ultrasound speckle tracking imaging. *J Am Coll Cardiol* 45: 2034–2041, 2005.
13. **Park TH, Nagueh SF, Khoury DS, Kopelen HA, Akrivakis S, Nasser K, Ren G, Frangogiannis NG.** Impact of myocardial structure and function postinfarction on diastolic strain measurements: implications for

assessment of myocardial viability. *Am J Physiol Heart Circ Physiol* 290: H724–H731, 2006.

14. **Popović ZB, Benejam C, Bian J, Mal N, Drinko J, Lee K, Forudi F, Reeg R, Greenberg NL, Thomas JD, Penn MS.** Speckle tracking echocardiography correctly identifies segmental left ventricular dysfunction induced by scarring in a rat model of myocardial infarction. *Am J Physiol Heart Circ Physiol* 292: H2809–H2816, 2007.
15. **Sebag IA, Handschumacher MD, Ichinose F, Morgan JG, Hataishi R, Rodrigues AC, Guerrero JL, Steudel W, Raher MJ, Halpern EF, Derumeaux G, Bloch KD, Picard MH, and Scherrer-Crosbie M.** Quantitative assessment of regional myocardial function in mice by tissue Doppler imaging: comparison with hemodynamics and sonomicrometry. *Circulation* 111: 2611–2616, 2005.
16. **Suffoletto MS, Dohi K, Cannesson M, Saba S, Gorcsan J, 3rd.** Novel speckle-tracking radial strain from routine black-and-white echocardiographic images to quantify dyssynchrony and predict response to cardiac resynchronization therapy. *Circulation* 113: 960–968, 2006.
17. **Thibault H, Gomez L, Donal E, Pontier G, Scherrer-Crosbie M, Ovize M, Derumeaux G.** Acute myocardial infarction in mice: assessment of transmurality by strain rate imaging. *Am J Physiol Heart Circ Physiol* 293: H496–H502, 2007.
18. **Thomas JD, Popovic ZB.** Speckle tracking echocardiography. In: *Braunwald's Heart Disease* (7th ed.), edited by Zipes DP, Libby P, Bonow RO and Braunwald E. Amsterdam: Elsevier, 2006.
19. **Uitenbroek DG.** *Correlations*. *SISA*. (online). http://www.quantitativeskills.com/sisa/statistics/correl.htm [1 July 2009].
20. **van den Bosch BJ, Lindsey PJ, van den Burg CM, van der Vlies SA, Lips DJ, van der Vusse GJ, Ayoubi TA, Doevendans PA, Smeets HJ.** Early and transient gene expression changes in pressure overload-induced cardiac hypertrophy in mice. *Genomics* 88: 480–488, 2006.
21. **Yamada H, Mowrey KA, Popovic ZB, Kowalewski WJ, Martin DO, Thomas JD, Wallick DW.** Coupled pacing improves cardiac efficiency during acute atrial fibrillation with or without cardiac dysfunction. *Am J Physiol Heart Circ Physiol* 287: H2016–H2022, 2004.
22. **Yang XP, Liu YH, Rhaleb NE, Kurihara N, Kim HE, Carretero OA.** Echocardiographic assessment of cardiac function in conscious and anesthetized mice. *Am J Physiol Heart Circ Physiol* 277: H1967–H1974, 1999.
23. **Zhang Y, Takagawa J, Sievers RE, Khan MF, Viswanathan MN, Springer ML, Foster E, Yeghiazarians Y.** Validation of the wall motion score and myocardial performance indexes as novel techniques to assess cardiac function in mice after myocardial infarction. *Am J Physiol Heart Circ Physiol* 292: H1187–H1192, 2007.